AIP Applied Physics Letters

The effect of electron-electron interaction induced dephasing on electronic transport in graphene nanoribbons

Sina Soleimani Kahnoj, Shoeib Babaee Touski, and Mahdi Pourfath

Citation: Applied Physics Letters **105**, 103502 (2014); doi: 10.1063/1.4894859
View online: http://dx.doi.org/10.1063/1.4894859
View Table of Contents: http://scitation.aip.org/content/aip/journal/apl/105/10?ver=pdfcov
Published by the AIP Publishing

The effect of electron-electron interaction induced dephasing on electronic transport in graphene nanoribbons

Sina Soleimani Kahnoj,[1,b)] Shoeib Babaee Touski,[1,b)] and Mahdi Pourfath[1,2,a),b)]
[1]*School of Electrical and Computer Engineering, University of Tehran, P.O. Box 14395-515, Tehran, Iran*
[2]*Institute for Microelectronics, TU Wien, Gusshausstrasse 27–29/E360, 1040 Vienna, Austria*

(Received 9 July 2014; accepted 26 August 2014; published online 8 September 2014)

The effect of dephasing induced by electron-electron interaction on electronic transport in graphene nanoribbons is theoretically investigated. In the presence of disorder in graphene nanoribbons, wavefunction of electrons can set up standing waves along the channel and the conductance exponentially decreases with the ribbon's length. Employing the non-equilibrium Green's function formalism along with an accurate model for describing the dephasing induced by electron-electron interaction, we show that this kind of interaction prevents localization and transport of electrons remains in the diffusive regime where the conductance is inversely proportional to the ribbon's length. © *2014 AIP Publishing LLC*. [http://dx.doi.org/10.1063/1.4894859]

Since the discovery of single-layer graphene,[1] this two-dimensional material has attracted the attention of many scientists due to its outstanding electronic properties. Extremely high intrinsic carrier mobility[2] and excellent thermal conductivity[3] are some of the features that make graphene a promising alternative material for current silicon-based technology. Single-layer graphene is a gap-less material, which makes it particularly unsuitable for switching applications. However, an energy gap can be induced by tailoring a graphene sheet into nanoribbons.[4] Depending on the arrangements of carbon atoms along the ribbon edges, graphene nanoribbons (GNRs) can have edges with zigzag shapes, armchair, or a combination of these two. Armchair GNRs (AGNRs), unlike zigzag GNRs, show semiconducting behavior. The electronic band gap of AGNRs is inversely proportional to the ribbon's width.[5] In order to obtain a suitable band gap for switching applications, the width of GNRs must be scaled to extremely narrow widths $W < 10\,\text{nm}$.[5] In narrow GNRs, on the other hand, line-edge roughness (LER) plays an important role on electronic transport properties.[6–9]

Transport of carriers is ballistic in devices with channel lengths much smaller than the mean free path (MFP) of carriers $L \ll \lambda$, where L represents the channel length and λ is the MFP. In this regime, the conductance is independent of the channel length and is proportional to multiple of $G_0 = 2q^2/h$. LER in GNRs, however, results in back-scattering of electrons and the reduction of the conductance. Transport of carriers will be in the diffusive regime in devices with channel lengths larger than the MFP and coherence length $l_\phi, \lambda \ll L$, where l_ϕ is the coherence length. In the diffusive transport regime, the average transmission probability can be written as[9]

$$\langle T(E)\rangle = \frac{M(E)}{1 + L/\lambda(E)}, \tag{1}$$

where $M(E)$ is the number of active conduction channels. This leads to an inversely proportionality of the conductance with the channel length $\langle G\rangle \propto 1/L$. On the other hand, if the phase coherence length is larger than the channel length $\lambda \ll L \ll l_\phi$, incident and back-scattered wavefunctions can coherently interfere with each other and form localized states along the ribbon which is referred to as Anderson localization. In this regime, localized regions are formed along the ribbon and the transport of electrons will be mostly by the tunneling of electrons between these localized states. As a result, the conductivity exponentially decreases with the channel length[9,10]

$$\langle \ln(g)\rangle = -\frac{L}{\xi}, \tag{2}$$

where $g = G/G_0$ and ξ is a characteristic length, which is referred to as localization length. In devices longer than this characteristic length, localization of carriers will occur. Scattering mechanisms such as electron-phonon and electron-electron (e-e) interactions, however, can break the coherence of carriers which prevents the formation of localized states and exponential decrease of the conductivity. Due to weak electron-phonon scattering in graphene, e-e scattering is the main source of dephasing at high temperatures.[11] Although e-e interaction has been the subject of intensive study in graphene,[12,13] its dephasing effect on electronic transport in narrow GNRs has not yet been addressed.

Electrons in π bonds of p_z-orbitals in graphene are responsible for electronic conduction. A first nearest-neighbor tight-binding model is employed to describe the electronic bandstructure of GNRs. The hopping parameter between first nearest-neighbor carbon atoms is assumed to be $-2.7\,\text{eV}$. It is assumed that edge carbon atoms are passivated by hydrogen atoms which accordingly affect the bonding distances between carbon atoms at the edges. Under this condition, the bond lengths parallel to dimer lines at edges are shortened by 3.3%–3.5% for narrow GNRs which in turn result in 12% increase in the hopping parameter between π-orbitals.[5] LER is modeled by randomly adding or removing of atoms at the edges. LER is an statistical phenomena that can be described by an auto-correlation function[6,9,14]

[a)]Electronic mail: pourfath@ut.ac.ir and pourfath@iue.tuwien.ac.at
[b)]All author contributed equally.

$$R(x) = dW^2 \exp\left(-\frac{|x|}{dL}\right), \tag{3}$$

where dW is the fluctuation amplitude and dL is the roughness correlation length. To generate LER in spatial domain, the auto-correlation function is Fourier transformed to obtain the spectral function. A random phase with even parity is applied and followed by an inverse Fourier transformation. For the given geometrical and roughness parameters, many samples are created and the electronic characteristics of each sample are evaluated. By taking an ensemble average, the role of LER and e-e interaction on the average transport characteristics is investigated. The ratio of the standard deviation over the ensemble average of the transmission probability is used as a control parameter for convergence. Our results indicate that more than ~100 samples are needed to minimize the statistical noise.

The non-equilibrium Green's function method is employed to model transport of electrons in GNRs.[9] The retarded Green's function of the channel is given by $G = [(E + i\eta)I - H - U - \Sigma_s - \Sigma_d - \Sigma_{e\text{-}e}]^{-1}$, where η is an infinitesimally small positive quantity, U is the electrostatic potential energy obtained by solving the Poisson equation self consistently with the transport equations,[15] H is the Hamiltonian of the device, $\Sigma_{s/d}$ are the source and drain contact self energies, respectively, and $\Sigma_{e\text{-}e}$ represents the self-energy due to e-e interaction. Assuming elastic scattering and a momentum conserving scheme, the matrix elements of the e-e interaction self-energy can be written as[16]

$$\Sigma_{e\text{-}e}(i,j) = D_{e\text{-}e}(i,j)G(i,j), \tag{4}$$

where $D_{e\text{-}e}$ is matrix representing the strength of the e-e interaction. For a momentum conserving interaction, one has $D_{e\text{-}e}(i, j) = d_p$ for all i, j.[16] e-e scattering rate in graphene at room temperature has been reported to be in the order of 50 ps at an electron concentration of $10^{12}\,\text{cm}^{-2}$.[17] Using the relation $\hbar/\tau_{e\text{-}e} = \Im m\{\Sigma_{e\text{-}e}\}$, one can obtain an approximate value for the e-e interaction strength $d_p \sim 10^{-3}$. As the Green's function and self-energy depend on each other, a non-linear equation system is achieved which can be solved by iteration until a convergence criterion is achieved.[18]

Fig. 1 compares the local density of states (LDOS) with and without e-e interaction at two energies $E = 0.4$ eV and $E = 0.7$ eV. As shown in Figs. 1(a) and 1(c), in phase-coherent transport regime carriers are spatially localized due to coherent interference of the incident and reflected wavefunctions. At $E = 0.7$ eV, localization of carriers is weaker than that at $E = 0.4$ eV. This behavior can be explained by the Thouless relation stating that the ratio of the localization length to the MFP is approximately proportional to the number of available conducting channels $\xi/\lambda \propto M(E)$.[19] As shown in Fig. 2, the number of available subbands increases with energy and so is the localization length. Thus, localization is more pronounced at low energies. e-e interaction, however, randomizes the phase of electron wavefunction, resulting in disappearance of interference and localized states, see Figs. 1(b) and 1(d).

The effects of e-e interaction on the DOS and transmission probability are depicted in Fig. 3. Total DOS at each energy is given by Trace$[A]/(2\pi)$, where $A = -2\text{Im}[G]$ is the spectral function. Unlike coherent transport, transmission probability cannot be defined in phase-incoherent transport regime. For a fair comparison of the results of these two transport regimes, an effective transmission probability for phase-incoherent transport regime can be defined as $\bar{T}(E) = I(E)/(f_S(E) - f_D(E))$, where $I(E)$ is the current spectrum.[16] In the presence of LER, the DOS and the transmission probability are smaller than that of an AGNR with perfect edges. On the one hand, LER induces edge and midgap states. On the other hand, in phase coherent transport, LER results in backscattering of electron wavefunction and the gradual formation of localized states due to coherent interference of the incident and backscattered waves. LER, therefore, induces peaks in the DOS and transmission probability. e-e scattering, similar to other scattering mechanisms, broadens the DOS and averages the transmission probability. Furthermore, by including e-e interaction, localized states will disappear due to the incoherency introduced by this scattering mechanism and the DOS and the transmission probability are smoothed out. Due to van-hove singularities

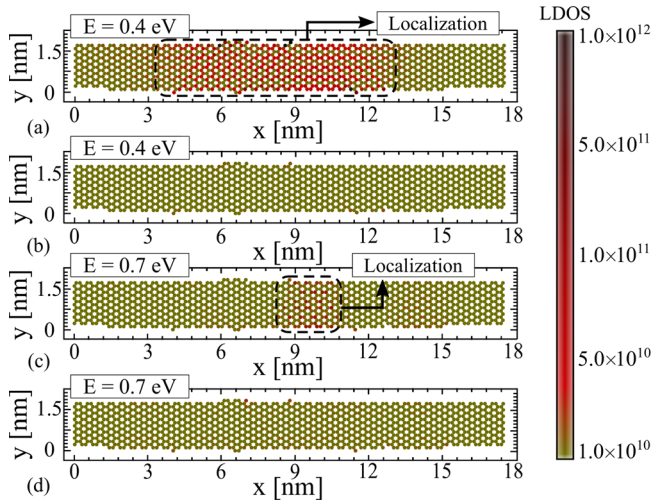

FIG. 1. The LDOS along a segment of a 50 nm AGNR with $nW = 15$, where nW is the number of carbon-dimmers along the width of the ribbon. $dW/W = 3\%$ and $dL = 5$ nm. (a) and (c) represent the results without e-e interaction, (b) and (d) are the results in the presence of e-e interaction. In the presence of phase breaking scattering, localized states disappear.

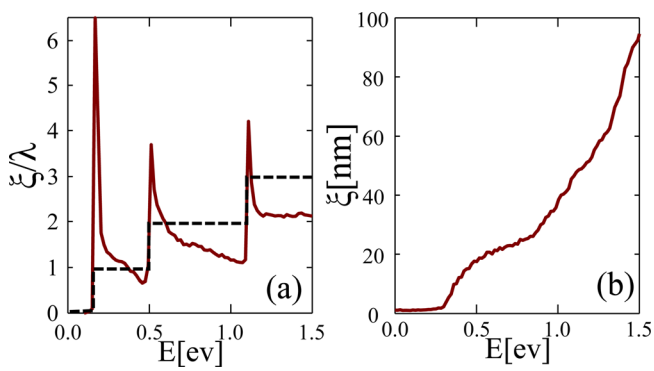

FIG. 2. (a) The ratio of the localization length to the MFP (solid line) and the number of conducting channels (dashed line) as functions of energy. (b) The localization length as a function of energy for rough ($dW/W = 3\%$ and $dL = 5$ nm) AGNRs with $nW = 15$. The results are in the absence of e-e interaction.

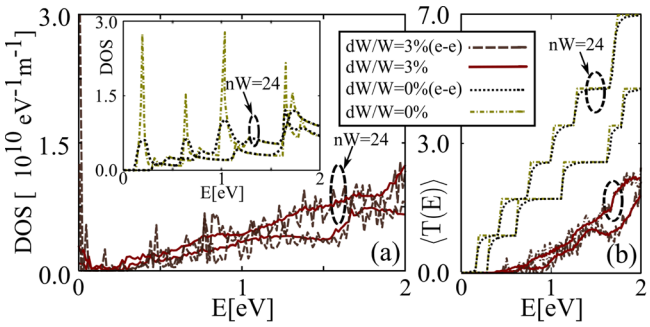

FIG. 3. (a) The DOS and (b) the transmission probability in the presence and absence of e-e interaction for rough ($dW/W = 3\%$ and $dL = 5$ nm) and perfect ($dW/W = 0\%$) AGNRs with $nW = 15$ and $nW = 24$ and a length of $L = 40$ nm. The results for AGNR with $nW = 24$ are denoted by dashed circles.

at the edge of each subband, the DOS and as a result the scattering rate increase considerably. Thus, the DOS and transmission probability are more smeared at such energies.

In the diffusive transport regime, one can evaluate the MFP (λ) by fitting a curve similar to Eq. (1) to the average transmission probability. The dependency of the MFP on the roughness amplitude for a short and long AGNR is compared in Fig. 4. Based on Fermi's golden rule, $\lambda \propto 1/dW^2$.[6,9] This trend is clearly observed for the AGNR with a short channel length, see Fig. 4(a), where transport is in the diffusive regime. In the presence of e-e interaction, the same trend is observed; however, small deviation can be seen at small roughness amplitudes. The total MFP can be defined as $1/\lambda = 1/\lambda_{\mathrm{LER}} + 1/\lambda_{\mathrm{e\text{-}e}}$, where λ_{LER} and $\lambda_{\mathrm{e\text{-}e}}$ are the MFPs for LER and e-e interaction, respectively. At small roughness amplitudes, the total MFP is dominated by e-e interaction, whereas at larger roughness amplitudes the MFP is dominated by LER and the expected trend is followed. One should note that the MFP is defined in the diffusive transport regime and does not depend on the channel length. However, as the channel length increases, localization of carriers occurs which in turn significantly reduces the transmission probability and conductance. As the MFP is evaluated from the transmission probability (Eq. (1)), the extracted effective MFP decreases in the presence of localization. As shown in Fig. 4(b), in a device with a longer channel length, localization occurs at smaller values of dW/W and the role of e-e on the total MFP is not observed.

Fig. 4(b) indicates that for phase-coherent transport, the dependency of the MFP with the roughness amplitudes deviates from $\lambda \propto 1/dW^2$ at larger roughness amplitudes. This behavior is attributed to the creation of localized states along the channel which results in exponential decrease of the conductance. In the presence of e-e interaction, however, these states are removed and electron transport will be in the diffusive regime. As a result, in the presence of e-e interaction, the MFP follows the results obtained from Fermi's golden rule. Fig. 5(a) depicts the average transmission as a function of the channel length at $E = 0.6$ eV. The results indicate that e-e interaction significantly increases the transmission probability and conductance in long channel AGNRs where electrons are localized, see Fig. 5(b). As shown in the inset of Fig. 5(a), the increase of e-e scattering rate results in shorter phase relaxation lengths and longer localization lengths.

To clarify the localization-diffusive crossover in the presence of e-e interaction, we discuss the conductance histogram and fluctuation in both the diffusive regime and localization regime. Conductance histograms in the diffusive transport regime are described by a Gaussian distribution function and the standard deviation is independent of the electron energy.[10] In other words, the conductance fluctuation in the diffusive regime is universal. In the localization regime, however, the histograms are not Gaussian, but they can be described by a log-normal distribution function. Furthermore, the conductance fluctuation is no longer universal, unlike the diffusive regime.[10] Fig. 6 shows the conductance histograms at two different energies. In the absence of e-e, all the histograms are described by log-normal distribution functions which represent localization regime. Fig. 6(b) shows that in presence of e-e interaction, the histograms become Gaussian that characterizes diffusive transport. It should be noted that the crossover between the localization and diffusive regime is not sharp and diffusive transport occurs when the channel length is much smaller than the localization length.

The effect of e-e interaction on electronic transport in AGNRs is theoretically studied. Due to the dephasing

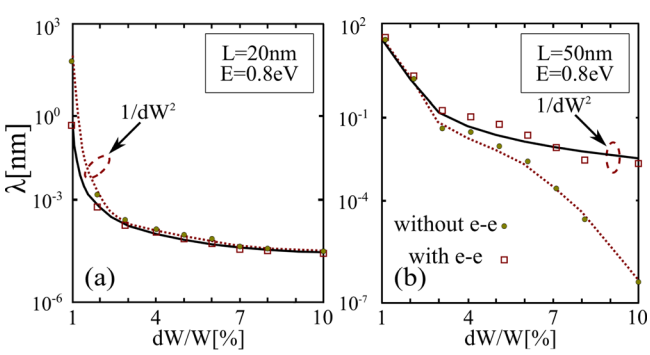

FIG. 4. The dependency of the MFP (λ) with roughness amplitude in the presence and absence of e-e interaction for AGNR with (a) $L = 20$ nm and (b) $L = 50$ nm. Because of the localization of electrons in phase-coherent transport at large roughness amplitudes and long channel lengths, the dependency of the MFP with roughness amplitude deviates from the expected value obtained from Fermi's golden rule. Dephasing induced by e-e interaction destroys localized states and results in the expected trend for the MFP.

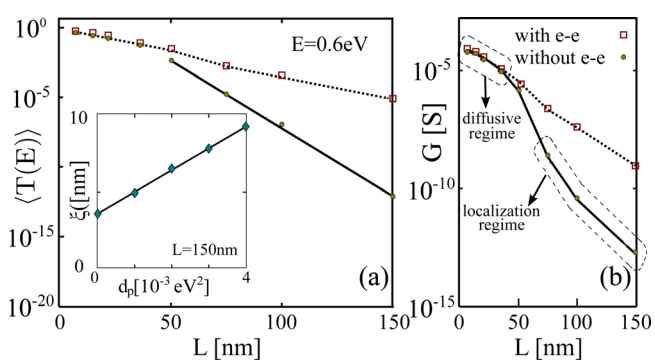

FIG. 5. The average (a) transmission probability and (b) conductivity as a function of length in the presence and absence of e-e interaction for AGNR with $nW = 15$, $dW/W = 3\%$, and $dL = 5$ nm. In the localization regime the transmission and resistivity increase exponentially with the length, whereas in the presence of e-e interaction the trend for diffusive regime is recovered. The inset shows localization length versus dephasing strength $E = 0.6$ eV. The localization length is extracted based on the approach described in Ref. 9.

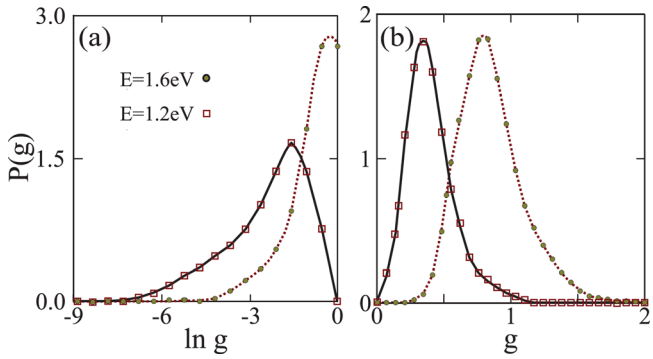

FIG. 6. The conductance ($g = G/G_0$) histograms in the (a) absence and (b) presence of e-e interaction at $E = 1.2$ eV and $E = 1.6$ eV. $L = 150$ nm, $dW/W = 3\%$, and $dL = 5$ nm. In the localization regime (a), the histograms are described by log-normal distribution functions, whereas in the diffusive transport regime (b) they are described a Gaussian one. In the diffusive transport regime, unlike localization, the conductance fluctuation is universal.

induced by e-e interaction, localized states in disordered AGNRs disappear, transport will be in the diffusive regime, and the expected results from Fermi's golden rule are recovered. The results indicate the importance of including e-e interaction for careful analysis of AGNRs with disorder.

The computational results presented have been achieved in part using the Vienna Scientific Cluster (VSC).

[1]K. S. Novoselov, A. K. Geim, S. Morozov, D. Jiang, Y. Zhang, S. Dubonos, I. Grigorieva, and A. Firsov, Science **306**, 666 (2004).
[2]F. Schedin, A. Geim, S. Morozov, E. Hill, P. Blake, M. Katsnelson, and K. Novoselov, Nat. Mater. **6**, 652 (2007).
[3]A. A. Balandin, S. Ghosh, W. Bao, I. Calizo, D. Teweldebrhan, F. Miao, and C. N. Lau, Nano Lett. **8**, 902 (2008).
[4]C. Berger, Z. Song, X. Li, X. Wu, N. Brown, C. Naud, D. Mayou, T. Li, J. Hass, A. N. Marchenkov *et al.*, Science **312**, 1191 (2006).
[5]Y.-W. Son, M. L. Cohen, and S. G. Louie, Phys. Rev. Lett. **97**, 216803 (2006).
[6]T. Fang, A. Konar, H. Xing, and D. Jena, Phys. Rev. B **78**, 205403 (2008).
[7]Y. Yang and R. Murali, IEEE Electron Device Lett. **31**, 237 (2010).
[8]A. Yazdanpanah, M. Pourfath, M. Fathipour, H. Kosina, and S. Selberherr, IEEE Trans. Electron Devices **58**, 3725 (2011).
[9]A. Yazdanpanah, M. Pourfath, M. Fathipour, H. Kosina, and S. Selberherr, IEEE Trans. Electron Devices **59**, 433 (2012).
[10]K. Takashima and T. Yamamoto, Appl. Phys. Lett. **104**, 093105 (2014).
[11]F. V. Tikhonenko, A. A. Kozikov, A. K. Savchenko, and R. V. Gorbachev, Phys. Rev. Lett. **103**, 226801 (2009).
[12]A. Sinner and K. Ziegler, Phys. Rev. B **82**, 165453 (2010).
[13]M. Schütt, P. Ostrovsky, I. Gornyi, and A. Mirlin, Phys. Rev. B **83**, 155441 (2011).
[14]S. Kim, M. Luisier, A. Paul, T. B. Boykin, and G. Klimeck, IEEE Trans. Electron Devices **58**, 1371 (2011).
[15]M. Pourfath and H. Kosina, *Large-Scale Scientific Computing*, Lecture Notes Computer Science Vol. 3743 (Springer, 2006), pp. 578–585.
[16]R. Golizadeh-Mojarad and S. Datta, Phys. Rev. B **75**, 081301 (2007).
[17]X. Li, E. Barry, J. Zavada, M. B. Nardelli, and K. Kim, Appl. Phys. Lett. **97**, 082101 (2010).
[18]M. Pourfath, *The Non-Equilibrium Green's Function Method for Nanoscale Device Simulation*, (Springer-Verlag, New York, 2014).
[19]D. J. Thouless, J. Phys. C: Solid State Phys. **6**, L49 (1973).